Journal of Thermal Analysis and Calorimetry, Vol. 67 (2002) 153–161

A KINETIC ASPECT OF THE THERMAL DEHYDRATION OF DILITHIUM TETRABORATE TRIHYDRATE

N. Koga[1]*, J. M. Criado*[2] *and H. Tanaka*[1]

[1]Chemistry Laboratory, Faculty of Education, Hiroshima University, 1-1-1 Kagamiyama, Higashi-Hiroshima 739-8524, Japan
[2]Instituto de Ciencia de Materiales, C.S.I.C.-Universidad de Sevilla, Sevilla 41092, Spain

Abstract

The reaction process of the thermal dehydration of dilithium tetraborate trihydrate, $Li_2B_4O_7 \cdot 3H_2O$, was reinvestigated from a viewpoint of reaction kinetics. On the basis of the results of thermogravimetry, constant rate thermal analysis, powder X-ray diffractometry, infrared spectroscopy and scanning electron microscopy, it was confirmed that the reaction proceeds via three consecutive kinetic steps characterized by different activation energies. The first and second kinetic steps, accompanied by the destruction of the original crystal structure of the reactant, seem to be assigned to the surface and internal reactions, respectively. During the third kinetic step, the thermal dehydration of hydrated amorphous intermediate, produced at the second kinetic step, and crystallization of the final dehydration product, $Li_2B_4O_7$, are likely to take place concurrently.

Keywords: CRTA, kinetics, $Li_2B_4O_7 \cdot 3H_2O$, TG, thermal dehydration

Introduction

Dilithium tetraborate trihydrate, $Li_2B_4O_7 \cdot 3H_2O$, can be utilized as a precursor of glassy and crystalline $Li_2B_4O_7$, known as the fast ionic conductor [1, 2]. The crystal structure of $Li_2B_4O_7 \cdot 3H_2O$ was solved from powder diffraction data, allowing to determine its structural formula as $Li(H_2O)B_2O_3(OH)$ [3]. The thermal dehydration process was studied by means of TG and DSC [4, 5]. On the basis of the crystal structure of the reactant and the reaction stoichiometry evaluated by thermal analysis, it was suggested that the thermal dehydration to crystalline $Li_2B_4O_7$ proceeds via $LiB_2O_3(OH)$ and an amorphous $Li_2B_4O_7$ [4, 5].

Recently, $Li_2B_4O_7 \cdot 3H_2O$ was successfully used as the precursor of crystalline $Li_2B_4O_7$ for preparing glassy $Li_2B_4O_7$ and studying the crystallization kinetics in $Li_2B_4O_7$ glass [6, 7]. Through these studies, it was found that TG and DTA curves for the thermal dehydration of $Li_2B_4O_7 \cdot 3H_2O$ do not indicate a smooth single step reaction but change systematically with the heating rate ϕ applied. It was assumed that the complicated behavior of the TG and DTA curves result from the kinetic feature of the thermal dehydration. In the present study, the reaction process of the thermal dehy-

1418–2874/2002/ $ 5.00

Akadémiai Kiadó, Budapest
Kluwer Academic Publishers, Dordrecht

dration of $Li_2B_4O_7 \cdot 3H_2O$ was reinvestigated from a viewpoint of kinetics in order to obtain a fundamental data for using $Li_2B_4O_7 \cdot 3H_2O$ as a precursor of crystalline $Li_2B_4O_7$.

Experimental

By slow evaporation of water vapor at 300 K with mechanical stirring, precipitates were obtained from a mixed solution of LiOH and H_3BO_3 in a fixed ratio of 1:2. The precipitates were dried at 400 K for 24 h and stored in a vacuum desiccator. Ratio of Li and B in the sample was determined by coupled neutralization titration as 2.01±0.02. The sample was identified by powder X-ray diffraction (XRD), Fourier transform infrared spectroscopy (FT-IR) and simultaneous TG-DTA. XRD pattern was recorded with a RINT2200 (Rigaku) using monochromed CuK_α radiation (40 kV, 20 mA). FT-IR was measured by diffuse reflectance using a FTIR-8100M (Shimadzu) for the samples mixed with KBr (3 mass% sample with 97 mass% KBr). TG-DTA measurements were performed using a TGD-7600 (ULVAC) at a heating rate of 10 K min^{-1} under flowing N_2 (80 mL min^{-1}). The samples lightly coated by Au evaporation were observed by scanning electron microscopy (SEM) using a JSM-T20 (Jeol).

The mass-loss processes of the sample at various heating rates ϕ were recorded using a Shimadzu TGA-50 under flowing N_2 (80 mL min^{-1}). Constant rate thermal analysis (CRTA) measurements under reduced pressure were performed using an instrument of the Rouquerol type [8], constructed using a thermobalance (Cahn2000) and a vacuum pumping system [9, 10]. The residual pressure during CRTA measurements, under dynamic vacuum at a constant pumping rate, was monitored by a penning gauge. The decomposition rate was controlled by regulating the sample temperature so as to maintain the residual pressure constant during the dehydration reaction. The sample dehydrated partially in the CRTA was collected and subjected to XRD and SEM.

Results and discussion

The recorded XRD pattern of the sample corresponded closely to that reported as $LiB_2O_3(OH) \cdot H_2O$ [3]. Figure 1 shows typical TG-DTA curves for the sample of 20.0 mg. Although DTA and DTG curves indicated several distinguished peaks during the mass-loss process, the total mass-loss of 24.4±0.3% was in good agreement with the theoretical value (24.2%) calculated by assuming the following dehydration reaction: $Li_2B_4O_7 \cdot 3H_2O \rightarrow Li_2B_4O_7 + 3H_2O$. A broad exothermic peak at the end of the dehydration seems to be due to the crystallization of poorly crystallized dehydration product. The sharp endothermic peak at a temperature of 1183.9±0.3 K corresponds to the melting of the $Li_2B_4O_7$ crystals [11]. Such thermal behavior is in good agreement with those reported by Touboul and Betourne [4, 5].

Influence of applied ϕ on the TG and DTG curves for the thermal dehydration process is shown in Fig. 2. It is seen from Fig. 2 that TG curves do not show a smooth

single step mass-loss and several peaks and shoulders are observed on DTG curves. Under linearly increasing temperature, the dehydration initiates at around 400 K with a gradual mass-loss. The dehydration is accelerated suddenly, accompanying with a

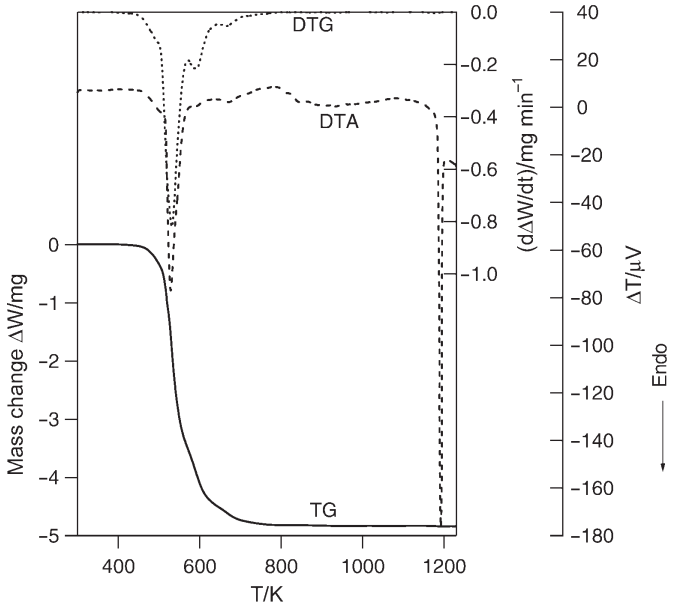

Fig. 1 Typical TG-DTA curves for the thermal dehydration of $Li_2B_4O_7 \cdot 3H_2O$ (20.0 mg) at ϕ=10 K min^{-1} under flowing N_2 at a rate of 50 mL min^{-1}

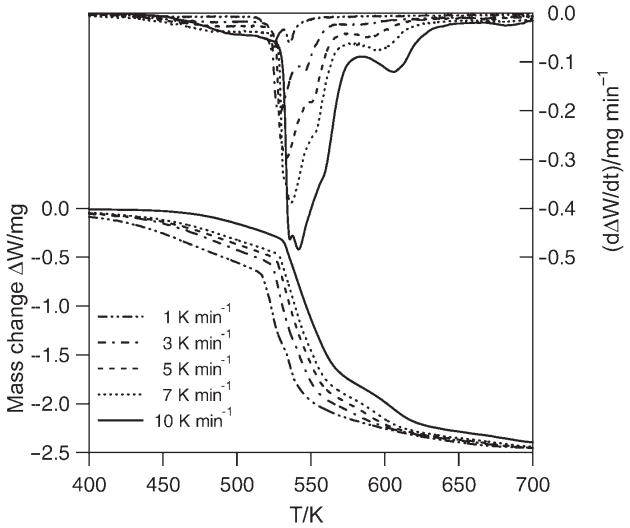

Fig. 2 Influence of ϕ on the TG-DTG curves for the thermal dehydration of $Li_2B_4O_7 \cdot 3H_2O$ (10.0 mg) under flowing N_2 at a rate of 50 mL min^{-1}

large DTG peak, at the fractional reaction α of 10–30% and around 520–540 K, followed by a decelerating process for the second half of the reaction. At the final part of the dehydration, an alternative DTG peak can be observed for the dehydration under larger heating rate ϕ. It is worth noting that the shapes of TG and DTG curves during the course of reaction change systematically with ϕ applied. Such a ϕ-dependent change in the overall behavior of the reaction indicates that the complicated behavior of the TG and DTG curves results from the influence of the kinetics and the mechanism of the dehydration. It is expected that the kinetic interpretation of the thermal dehydration helps us to understand the thermal dehydration process with a wider comprehension.

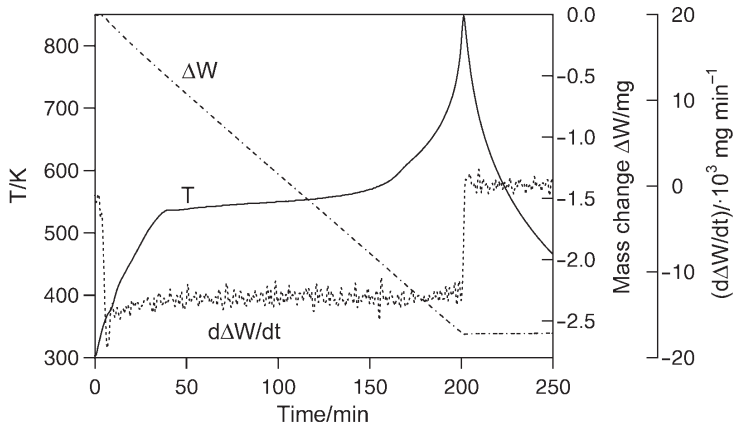

Fig. 3 Typical CRTA curves recorded at the controlled pressure of $4.0 \cdot 10^{-3}$ Pa under the basal pressure of $2.0 \cdot 10^{-3}$ Pa for the thermal dehydration of $Li_2B_4O_7 \cdot 3H_2O$ (10.7 mg)

Figure 3 shows typical CRTA traces for the thermal dehydration under reduced pressure. The change in the dehydration behavior observed on the conventional TG and DTA curves is also seen clearly here from the change in the temperature profile under constant rate dehydration during the course of reaction. A nearly linear increase of the temperature is observed at the initial part of the reaction. At around α=20%, an abrupt bend of the reaction temperature is seen and subsequently the temperature increases very slowly with the reaction proceeds. After passing ϕ=80%, the temperature starts to increase rapidly to maintain the reaction rate constant.

A series of CRTA curves recorded, for the thermal dehydration of the sample with different mass, at a controlled pressure of $1.0 \cdot 10^{-2}$ Pa under the basal pressure of $2.0 \cdot 10^{-3}$ Pa are shown in Fig. 4. With the increasing sample mass, the reaction temperature decreases systematically due to the following relationship among the controlled rate C (expressed in mg min^{-1}), the total mass-change Δm (expressed in mg) and the normalized reaction rate $d\alpha/dt$: $(d\alpha/dt)=C/\Delta m$. Thus, provided that the reaction rate C has been maintained constant at the whole set of experiments, the higher the starting sample mass is, the lower the normalized decomposition rate ($d\alpha/dt$) is, and therefore, the lower the reaction temperature is. From the relationship of the reaction temperature and the reduced reaction

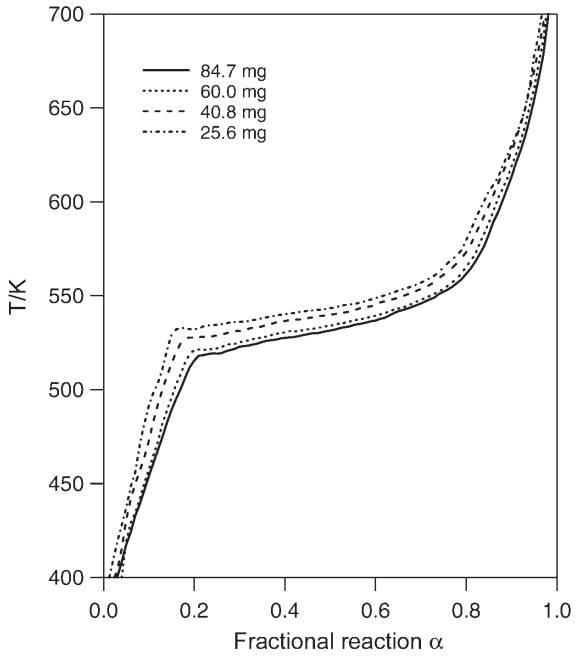

Fig. 4 Influence of sample size on the temperature profile of the constant rate thermal dehydration of $Li_2B_4O_7{\cdot}3H_2O$ recorded at the controlled pressure of $1.0{\cdot}10^{-2}$ Pa under the basal pressure of $2.0{\cdot}10^{-3}$ Pa

rate, apparent values of activation energy, E, at various selected α can be determined by Friedman plot [12], according to the following equation.

$$\ln\left(\frac{d\alpha}{dt}\right) = \ln[Af(\alpha)] - \frac{E}{RT} \quad (1)$$

Figure 5 shows typical Friedman plots at various selected α. Fairly linear correlations between $\ln(d\alpha/dt)$ and T^{-1}, with the correlation coefficient of the linear regression analysis γ better than –0.98, were observed in a wide range of the selected α from 0.06 to 0.99. The slope of the Friedman plots change depending on α. The α-dependence of the apparent value of E, calculated from the slope of the Friedman plots at various α, is shown in Fig. 6. It is apparent that three distinguished ranges of α characterized by different values of E, 77.6±5.0 kJ mol^{-1} (α<0.20), 250.6±12.1 kJ mol^{-1} ($0.20 \leq \alpha \leq 0.75$), and 218.80±12.6 kJ mol^{-1} (α>0.75), can be identified. This finding indicates that the thermal dehydration of $Li_2B_4O_7{\cdot}3H_2O$ proceeds via, at least, three different kinetic steps.

Figure 7 shows typical XRD patterns of the samples dehydrated partially under the constant rate condition. The diffraction peaks of the reactant diminish as the reaction proceeds and disappear completely at about α=0.75. The reaction process of diminishing the diffraction peaks of the reactant corresponds to the range of α for the

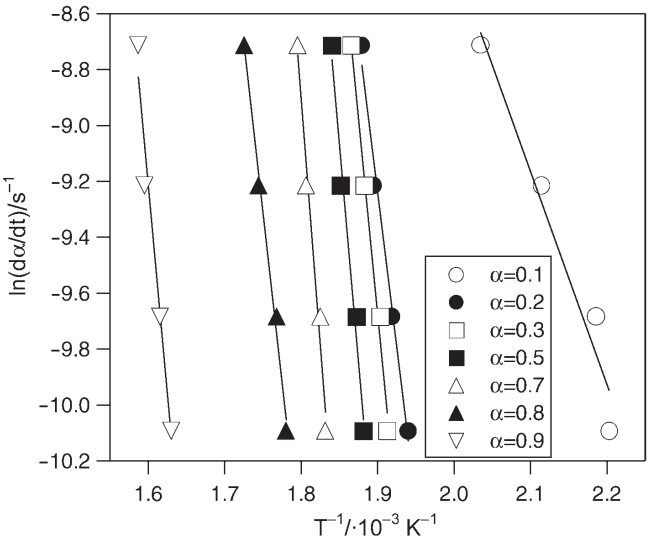

Fig. 5 Typical Friedman plots at various α for the constant rate thermal dehydration of $Li_2B_4O_7 \cdot 3H_2O$ under vacuum

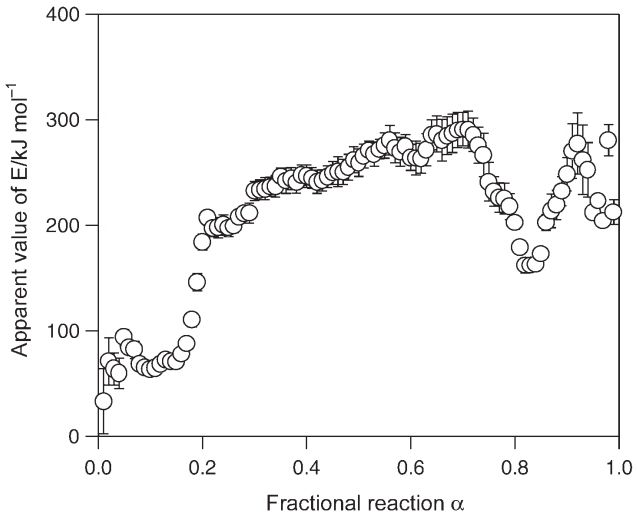

Fig. 6 Activation energies, *E*, at various α for the constant rate thermal dehydration of $Li_2B_4O_7 \cdot 3H_2O$ under vacuum

first and second kinetic steps described above. The subsequent process can be characterized by the growth of the diffraction peaks of the solid product, $Li_2B_4O_7$. The third kinetic process is described by the mass-loss process accompanied by the crystallization of the solid product. Figure 8 shows typical SEM images of the reactant and solid product of the thermal dehydration. The reactant is composed of the crystals of qua-

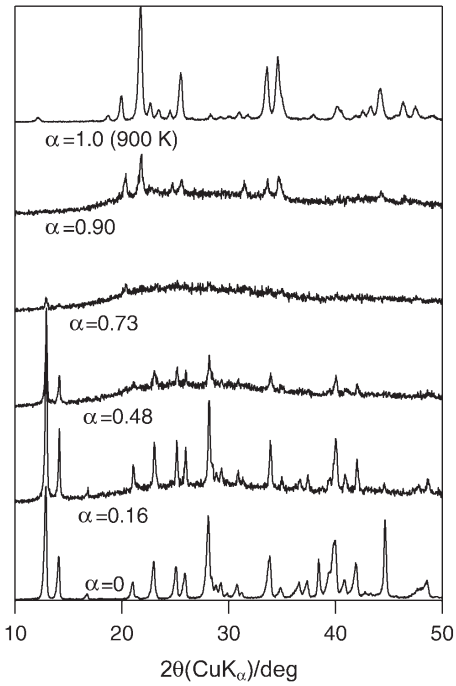

Fig. 7 Typical XRD patterns for the sample dehydrated partially in the CRTA

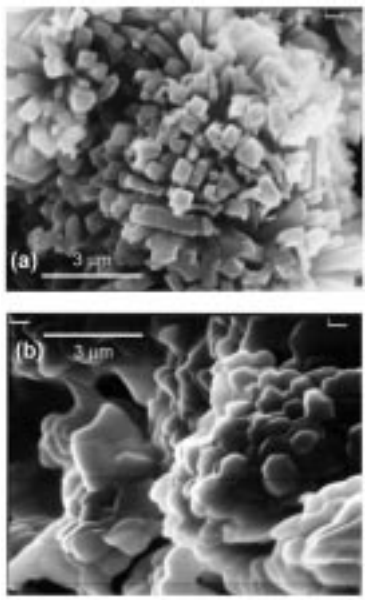

Fig. 8 Typical scanning electron microscopic views of a – the reactant, $Li_2B_4O_7 \cdot 3H_2O$, and b – the solid product of the thermal dehydration, $Li_2B_4O_7$

dratic prism (1 to 2 μm long and 0.2 to 0.5 μm wide). The superficial morphology observed by SEM did not change during the first and second kinetic steps of the reaction. The morphological change took place during the third kinetic step by forming sintered petal-like crystals of the solid product.

The results indicate that the steps of decomposition of the reactant and crystallization of the solid product take place at different times and separated in space. Generally, the thermal dehydration of solids initiates at the surface, followed by the advancement of the reaction interface inwards. During the initial part of the reaction, the reaction temperature under constant rate dehydration increases nearly linearly (Figs 3 and 4). Such a temperature profile during the early stage of reaction is in good agreement with the theoretically evaluated temperature profile for the diffusion controlled reaction model [13, 14]. Under such a condition, the diffusional removal of the water vapor produced at the reaction interface may become difficult and the partial pressure of water vapor at the reaction interface increases.

A sudden change in the temperature profile of the CRTA measurements observed at around α=0.2 seems to be described by a kind of crack formation on the surface layer of the solid product, which may provide a possible diffusion route of the evolved water vapor for the subsequent reaction. The similar reaction behavior has been reported for the thermal dehydration of various crystalline hydrates [15–18]. From the gradual increase of reaction temperature in the CRTA records, the second kinetic step is deduced to proceed by the shrinkage of reaction interface controlled by the chemical reaction, i.e., phase boundary controlled reaction [13, 14].

The intermediate solid-product just after the second kinetic step was amorphous in view of XRD (Fig. 7) and a broad IR absorption peak due to O–H stretching was observed in the range of 2500–3800 cm^{-1}. It is seen from Fig. 2 that the portion of the third kinetic step decreases with increasing the portion of the first kinetic step. Deducing from these results, a hydrated amorphous intermediate seems to be produced during the second kinetic step. The third kinetic step of the reaction proceeds by the dehydration of the amorphous intermediate, accompanied by the crystallization of solid product, $Li_2B_4O_7$.

Conclusions

The process of thermal dehydration of $Li_2B_4O_7 \cdot 3H_2O$ consists of three consecutive kinetic steps characterized by different activation energies, 77.6±5.0 (α<0.2), 250.6±12.1 (0.2≤α ≤0.75), and 218.8±12.6 kJ mol^{-1} (α>0.75), respectively. The first and second kinetic steps, which consist of the process of destroying the original crystal structure of the reactant, can be distinguished as surface and internal reactions, respectively. A hydrated amorphous intermediate seems to be produced through the second kinetic step. The third kinetic step is described as the thermal dehydration of the amorphous intermediate, accompanied by the crystallization of solid product, $Li_2B_4O_7$.

References

1 H. L. Tuller, D. P. Button and D. R. Uhlmann, J. Non-Cryst. Solids, 40 (1980) 93.
2 M. D. Ingram, Phys. Chem. Glasses, 28 (1987) 215.
3 D. Louer, M. Louer and M. Touboul, J. Appl. Cryst., 25 (1992) 617.
4 M. Touboul and E. Betourne, Solid State Ionics, 63-65 (1993) 340.
5 M. Touboul and E. Betourne, Solid State Ionics, 84 (1996) 189.
6 N. Koga, K. Yamaguchi and J. Šesták, J. Therm. Anal. Cal., 56 (1999) 755.
7 N. Koga and J. Šesták, J. Am. Ceram. Soc., 83 (2000) 1753.
8 J. Rouquerol, Thermochim. Acta, 144 (1989) 209.
9 F. Gotor, M. Macias, A. Ortega and J. M. Criado, Int. J. Chem. Kinetics, 30 (1998) 645.
10 N. Koga and J. M. Criado, Int. J. Chem. Kinetics, 30 (1998) 737.
11 B. S. R. Sastry and F. A. Hummel, J. Am. Ceram. Soc., 41 (1957) 7.
12 H. L. Friedman, J. Polym. Sci., Part C, 6 (1964) 183.
13 J. M. Criado, A. Ortega and F. Gotor, Thermochim. Acta, 157 (1990) 171.
14 L. A. Perez-Maqueda, A. Ortega and J. M. Criado, Thermochim. Acta, 277 (1996) 165.
15 A. K. Galwey, R. Spinicci and G. G. T. Guarini, Proc. R. Soc. London, Ser. A, 378 (1981) 477.
16 H. Tanaka and N. Koga, J. Phys. Chem., 92 (1988) 7023.
17 G. G. T. Guarini and M. Rustici, React. Solids, 6 (1988) 277.
18 N. Koga and H. Tanaka, J. Phys. Chem., 98 (1994) 10521.